

From Trees to Galaxies: The Potts Model on a Random Surface

Mark Wexler

*Niels Bohr Institute, Blegdamsvej 17
2100 Copenhagen Ø, Denmark
wexler@nbivax.nbi.dk*

Abstract

The matrix model of random surfaces with $c = \infty$ has recently been solved and found to be identical to a random surface coupled to a q -states Potts model with $q = \infty$. The mean field-like solution exhibits a novel type of tree structure. The natural question is, down to which—if any—finite values of c and q does this behavior persist? In this work we develop, for the Potts model, an expansion in the fluctuations about the $q = \infty$ mean field solution. In the lowest—cubic—non-trivial order in this expansion the corrections to mean field theory can be given a nice interpretation in terms of structures (trees and “galaxies”) of spin clusters. When q drops below a finite q_c , the galaxies overwhelm the trees at all temperatures, thus suppressing mean field behavior. Thereafter the phase diagram resembles that of the Ising model, $q = 2$.

1 Introduction

The infinite-state Potts model on random spherical surface can be solved exactly [1, 2] by resumming all orders of its low temperature expansion [3]. The problem and its solution are of interest for the following reasons.

- It can be shown to be equivalent to conformally invariant models with $c = \infty$ (which can be realized, for example, by coupling multiple Ising models to the surface). Thus the solution opens a window onto the mysterious $c > 1$ regime, hitherto inaccessible via either Liouville theory or matrix models.
- This equivalence to conformal matter holds in spite of a well known fact that on a fixed two-dimensional lattice a Potts model with more

that four states suffers a first order—rather than a continuous—phase transition. Coupling an ∞ -state Potts model to a random surface changes the order of the transition from first to third; in the case of $q < 4$ the order of the transition correspondingly changes from second to third.

- The reason why the transition for $q = \infty$ is of third order is that it is no longer a spin-ordering transition; rather it is a tree-growing transition, where the nodes of the trees are spin clusters (equivalently, “baby universes”). The transition in the random surface Potts model from spin-ordering (low q) to tree-growing (high q) behavior is a novel one, and deserves attention in its own right.

Some recent work has given support to the mean field theory at $q = c = \infty$. Ambjørn, Durhuus and Jónsson [4, 5] (see also [6]) have shown that if a random surface model has susceptibility exponent γ_{str} , its “polymerized” version has $\bar{\gamma}_{\text{str}} = \gamma_{\text{str}}/(\gamma_{\text{str}} - 1)$, in agreement with the mean field result $\bar{\gamma}_{\text{str}} = \frac{1}{3}$. Their polymerized surfaces of baby universes are suggestive of the trees of clusters found in the mean field model.¹ Harris and Wheeler [7] have studied multiple Ising models, and in the limit $c \rightarrow \infty$ have identified trees as dominant, and found $\gamma_{\text{str}} = \frac{1}{2}$.² A recent numerical study [8] of multiple $q = 2, 3$, and 4 Potts models shows that spikiness of the surfaces increases with increasing central charge, and that γ_{str} may well approach $\frac{1}{3}$. Finally, a current numerical study of the Potts model for various values of q and for surfaces with tadpoles and self-energies [9] is confirming the scaling of the critical temperature $T_c^{-1} = \frac{1}{2} \log q + \mathcal{O}(1)$ with large q , and, more significantly, details of cluster geometry predicted by the mean field theory.

For convenience, let us introduce the concept of a *skeleton graph*: given a triangulated surface with some spin configuration, its skeleton is a graph that represents the spin clusters as simple vertices, and whose edges are the links between different spin clusters.³ Each loop of skeleton graph introduces a factor $1/q$ (or $1/c$ for conformal models). Thus at $q = \infty$ (or at $c = \infty$), the only skeletons that are present are trees. When we move down to large

¹Although baby universes (geometrical structures) are not *a priori* identical to clusters (matter structures), the two seem to fuse at large q or c . Note that the trees in [4] are a result of the $N \rightarrow \infty$ limit, while the trees in [1, 2] are a result of $q, c \rightarrow \infty$.

²Their trees are made of *vertices*, not *clusters*, and thus form a subset of trees-of-clusters. There is no contradiction: to find clusters at the vertices of the trees, one has to take $c \rightarrow \infty$ and $T \rightarrow 0$ simultaneously, keeping $e^{-2/T}c$ fixed.

³So be definition, no vertex of a skeleton may be connected to itself.

but finite q , the corrections introduce loops; and while the leading terms are universal, the corrections in $1/q$ are not—their details depend on the details of the matter model. This is a familiar picture in $1/D$ expansions. For instance in the scalar $\lambda\phi^4$ theory, the upper critical dimension is 4: below this, fluctuations or “loops” become essential, and mean field theory breaks down.

It would be very interesting to know if something similar happens for random surfaces. One’s curiosity is heightened by the fact that Liouville theory seems to be silent on the matter. To investigate the large-but-finite q region, we develop a systematic expansion of the model (in its equivalent one-matrix form) about the $q = \infty$ solution. A priori, we would expect that the first non-trivial order in this expansion to be quadratic, as in many similar cases. In this order we sum all the skeletons that have one or no loops, in other words the q^0 and q^{-1} terms in the partition function. But it is not hard to show that this q^{-1} correction is insignificant, in that it does not modify the critical behavior of the model.

The next, cubic, order of our approximation is much richer. Here we include all skeletons whose clusters have three or fewer external legs that lie on loops. We therefore have terms with arbitrarily many loops, meaning arbitrarily high powers of q^{-1} . A new structure makes its appearance: the clusters are organized into ϕ^3 graphs of spherical topology. These “surfaces” of clusters will be called *galaxies*. The trees are still present: any number of them may grow out of any cluster. On top of that, a typical skeleton graph includes several galaxies, linked also into a tree.

This complicated system shows complicated critical behavior. For $q = \infty$, there is a magnetized low temperature phase where the clusters are large, and there are few of them: essentially pure gravity. At some point that phase becomes unstable, and the tree of clusters blows up. Above that, the clusters are small, but the tree is large.

At large but finite q , the above picture of critical behavior is unchanged, except for the appearance of a new phase at high temperature, that of large galaxies. At low temperature we still have the pure gravity phase of large clusters; this still goes into an intermediate phase of large trees. But now, at an even higher temperature (which is infinite when q is infinite, and which decreases with q), the area of the galaxies—the number of clusters they contain—diverges. In this phase, the loops become essential: without loops there could be no galaxies. The phase of large galaxies is also akin to pure gravity.

The tree phase becomes narrower and narrower as q decreases, until at some q_c , it disappears altogether: one goes from the magnetized phase directly into the phase of large galaxies. Although mean field theory is modified at any finite q , it is completely destroyed below q_c . For $q \leq q_c$ the phase diagram is altogether reasonable, in that it resembles the known phase diagrams of the $q < 4$ models: there are two pure gravity phases, at low and at high temperature, separated by a multicritical point.

This paper is organized as follows. Section 2 presents the multi-matrix version of the Potts model, its low temperature expansion, its effective one-matrix versions, and its $q = \infty$ solution. In section 3 we introduce an expansion about the $q = \infty$ solutions and its truncated versions, and discuss its geometrical implications. In section 5 we analyze the critical behavior of the simplest nontrivial truncation.

2 Definition of the model

The q -state Potts model on a spherical random surface will be defined using a matrix model (see [10] for a review):

$$F_q(g, \zeta) = \frac{1}{q} \log \frac{1}{f_0} \int \mathcal{D}\phi_1 \cdots \mathcal{D}\phi_q \exp -N \text{Tr} \left(\frac{1}{2} \sum_{ij} \phi_i G_{ij} \phi_j + g \sum_i \phi_i^3 \right) \quad (1)$$

where the ϕ_i are $N \times N$ hermitian matrices and all matrix integrals are to be understood as being divided by N^2 and taken in the limit $N \rightarrow \infty$. The matrix G defines the matter that is to be coupled to the fluctuating surface; in the case of the Potts model it is

$$G = \begin{pmatrix} 1 & \zeta & \cdots & \zeta \\ \zeta & 1 & \ddots & \vdots \\ \vdots & \ddots & \ddots & \zeta \\ \zeta & \cdots & \zeta & 1 \end{pmatrix}^{-1} = \begin{pmatrix} a_q & b_q & \cdots & b_q \\ b_q & a_q & \ddots & \vdots \\ \vdots & \ddots & \ddots & b_q \\ b_q & \cdots & b_q & a_q \end{pmatrix} \quad (2)$$

$$a_q = \frac{1 + (q-2)\zeta}{(1-\zeta)(1+(q-1)\zeta)}, \quad b_q = \frac{-\zeta}{(1-\zeta)(1+(q-1)\zeta)} \quad (3)$$

The coupling constant ζ is related to the matter temperature by $\zeta = e^{-2/T}$. Finally, the normalization f_0 is defined by requiring $F_q(0, \zeta) = 1$.

The partition function F_q can be expanded in powers of ζ . This is the so-called low temperature or cluster expansion, as in order ζ^n we have a

sum over all connected configurations of clusters with n inter-cluster links; as well as over the *internal* geometry of each cluster. Defining $\Delta = q - 1$, the first four orders of the expansion are

$$\begin{aligned}
F_q(g, c) = & \pi_0 + \frac{1}{2}\Delta\pi_1^2\zeta + \left[\frac{1}{2}\Delta^2\pi_1^2(\pi_2 + \pi_{11}) + \frac{1}{4}\Delta\pi_2^2 \right] \zeta^2 \\
& \bullet \quad \text{---} \bullet \quad \text{---} \text{---} \bullet \quad \text{---} \text{---} \text{---} \bullet \\
& + \left[\frac{1}{2}\Delta^3\pi_1^2(\pi_2 + \pi_{11})^2 + \frac{1}{6}\Delta^3\pi_1^3(\pi_3 + \pi_{12} + \pi_{111}) + \frac{1}{6}\Delta(\Delta - 1)\pi_2^3 \right. \\
& \quad \text{---} \text{---} \text{---} \bullet \quad \begin{array}{c} \bullet \\ | \\ \bullet \end{array} \quad \begin{array}{c} \bullet \\ / \quad \backslash \\ \bullet \end{array} \\
& + \frac{1}{2}\Delta^2\pi_1\pi_2 \left(\pi_3 + \frac{\pi_{12}}{3} \right) + \frac{1}{24}\Delta\pi_3^2 \left. \right] \zeta^3 + \dots \\
& \quad \text{---} \text{---} \text{---} \bullet \quad \text{---} \text{---} \text{---} \bullet \quad \text{---} \text{---} \text{---} \bullet
\end{aligned} \tag{4}$$

The picture underneath each term is the corresponding skeleton graph—see the Introduction. The various coefficients π_p (p is a partition of an integer n , where n is the cluster's external legs) are functions of the cosmological constant g that sum over the internal geometries of the clusters.

To define and to calculate the π 's, one introduces an external matrix integral

$$\Pi(g, \Lambda) = -\frac{1}{2N} \text{Tr} \Lambda^2 - \log \frac{1}{p_0} \int \mathcal{D}\phi \exp -N \text{Tr} \left(\Lambda\phi + \frac{1}{2}\phi^2 + g\phi^3 \right) \tag{6}$$

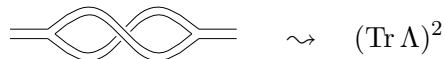
This integral has been calculated by Kazakov and by Gross and Newman. If we expand it in powers of Λ , we get

$$\begin{aligned}
\Pi(g, \Lambda) = & \pi_0 + \frac{\pi_1}{N} \text{Tr} \Lambda + \frac{1}{2} \left[\frac{\pi_2}{N} \text{Tr} \Lambda^2 + \frac{\pi_{11}}{N^2} (\text{Tr} \Lambda)^2 \right] \\
& + \left[\frac{\pi_3}{N} \text{Tr} \Lambda^3 + \frac{\pi_{12}}{N^2} \text{Tr} \Lambda \text{Tr} \Lambda^2 + \frac{\pi_{111}}{N^3} (\text{Tr} \Lambda)^3 \right] + \dots \tag{7}
\end{aligned}$$

The coefficients $\pi_p(g)$ are the ones we encounter in the low temperature expansion (4). In n -th order, we find π_p for all partitions p of n . The coefficient $\pi_{n_1 n_2 \dots}$ is a connected Green's function of the one-matrix model $\Pi(g, 0)$ with $n_1 + n_2 + \dots$ external legs, on each of which we place the matrix Λ ; the graphs can be twisted in various ways, which gives rise to the different combinations of traces. For example, π_2 sums graphs such as

$$\begin{array}{c} \text{---} \text{---} \text{---} \text{---} \end{array} \rightsquigarrow \text{Tr} \Lambda^2$$

while π_{11} sums graphs such as



$$\sim (\text{Tr } \Lambda)^2$$

The untwisted coefficients π_n are just the n -point connected BIPZ Green's function [11], while the twisted coefficients have not been discussed before in the literature. They can all be calculated exactly, and the first few are given in Appendix A.

The complicated linear combinations of the coefficients π_p appearing in the low temperature expansion (4) are due to the large N limit of our model. It will be seen below that there is a way to organize these linear combinations that will clarify their nature and simplify their calculation.

Here we briefly summarize the solution of the Potts model in the $q \rightarrow \infty$ limit. As it can easily be seen that the coefficient of ζ^n in the partition function is an n -th degree polynomial in Δ , the proper scaling for the temperature is $\zeta \sim 1/\Delta$. Defining $\zeta = a/\Delta$ and keeping a fixed⁴ while letting $q \rightarrow \infty$, it was found that only skeleton graphs that are trees contribute to $F_\infty(g, a)$. These can be resummed to give

$$F_\infty(g, a) = \lim_{\theta \rightarrow \infty} \frac{1}{\theta} \log \frac{1}{f_0} \int_{-\infty}^{\infty} dx \exp -\theta \left[\frac{x^2}{2a} - \Pi(g, x) \right] \quad (8)$$

$$= \Pi(g, y) - \frac{y^2}{2a}, \quad \Pi(g, y) \equiv \Pi(g, y1) \quad (9)$$

where the function $y(g, a)$ is a saddle point of F_∞ :

$$y = a \frac{\partial}{\partial y} \Pi(g, y) = a \Pi_1(g, y) \quad (10)$$

The general features of the $q = \infty$ model's critical behavior have already been described in the Introduction; see [2] for details.⁵

Kazakov [12] has pointed out that the random surface Potts model can also be formulated as a one-matrix model with the action

$$S_n = \Delta \left[\frac{1}{2\hat{a}} \text{Tr } \phi^2 - N \left(1 + \frac{1}{\Delta} \right) \Pi \left((1 - a/\Delta)^{3/2} g, \phi \right) \right], \quad \hat{a} = \frac{a}{1 - a/\Delta} \quad (11)$$

⁴This is the most interesting way of taking the $q \rightarrow \infty$ limit. If we keep ζ fixed instead, for example, we will find only one of the several phases of the model.

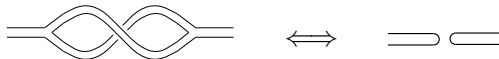
⁵This limit can be called a mean field solution because it can be arrived at by (an *a priori* inexact) procedure of substituting $\phi_i \phi_j \rightarrow \Phi \phi_i$ in the multi-matrix model (1) and solving self-consistently for Φ ; additionally, one has to take the (not *a priori* obvious) ansatz that Φ is a multiple of unity, as in Wilson's mean field solution of QCD.

The simple derivation is given in Appendix B. This effective action will be called the “natural” one. For the purposes of the present calculation, it is useful to introduce a slightly different, “artificial” effective action

$$S_a = \Delta \left[-\rho \text{Tr } \phi + \frac{1}{2a} \text{Tr } \phi^2 - N\Pi(g, \phi) \right] \quad (12)$$

The difference between these two effective models, their relative merits and drawbacks, are fully explained in Appendix B.

In going from the multi-matrix model (1) to the effective one-matrix models (11) and (12), we trade the complexity of having several matrices for the complexity of the new one-matrix potential—see eq. (7). But what is really happening is that the vertices of the effective models are playing a completely different role than the vertices of the original model. In the original multi-matrix model, the vertices represented points on the discretized worldsheet. In the effective models, the vertices—which are complicated functions of the original cosmological constant g —actually represent entire spin clusters. This is possible because a twisted cluster is equivalent, from the large- N fatgraph point of view, to a nonlinear vertex



such as $(\text{Tr } \Lambda)^2$. This is why all possible nonlinear terms appear in the expansion (7) of the potential $\Pi(g, \Lambda)$; or, seen from the other direction, why clusters of every possible twist appear in the low temperature expansion (4).⁶

One could rederive the $q, \Delta \rightarrow \infty$ limit in a quick and dirty way by noticing that when the model (11) is reduced to an eigenvalue problem, the charge of the eigenvalues will scale as Δ^{-1} , and therefore the width of the eigenvalue spectrum will scale as $\Delta^{-1/2}$. At $\Delta = \infty$, the eigenvalue density will be a delta function—precisely the content of equation (8).

3 Fluctuations about the mean field

So at $q = \infty$ the eigenvalue density of the effective models (11) and (12) collapses to a delta function. When q is large but finite, the eigenvalues

⁶The procedure that led from multi-matrix model to the effective one-matrix model can be applied to any—not only Potts—matter. Only the Potts model, however, is symmetric with respect to *any* relabeling of matter states; that is why its effective model is a *one*-matrix model. Effective cluster models for other types of matter are multi-matrix models.

spread into a narrowly peaked distribution. The main idea of this work is to investigate the shape of that distribution by expanding the effective models about the scalar solution

$$\phi = y1 + \psi \quad (13)$$

in powers of ψ . One type of critical point will result from singularities of the equations for the eigenvalue distribution of ψ . Once an approximate distribution is found in this way, we will plug it back into the full effective model to determine critical behavior; another type of critical point will result from singularities of the potential Π for a given ψ . For simplicity, the following calculations will be shown only for the artificial model (12); the calculations for the natural model (11) differ in trivial ways, and their result will be given at the end.

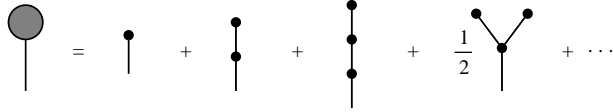
The action (12) now reads

$$S_a = \Delta \left[N \left(-\rho y + \frac{y^2}{2a} \right) + \left(-\rho + \frac{y}{a} \right) \text{Tr } \psi + \frac{1}{2a} \text{Tr } \psi^2 - N\Pi(g, y + \psi) \right] \quad (14)$$

The reader is reminded [2] that the $q = \infty$ partition function F_∞ is a sum over free trees, and its saddle point $y(g, a)$ is a sum over *planted* trees: trees with a marked vertex of order one. Explicitly,

$$y(g, a) = \pi_1 a + \pi_1 (\pi_2 + \pi_{11}) a^2 + \left[\pi_1 (\pi_2 + \pi_{11})^2 + \frac{1}{2} \pi_1^2 (\pi_3 + \pi_{12} + \pi_{111}) \right] + \dots \quad (15)$$

This low temperature expansion of y can be represented graphically as



We are led to consider the expansion of the external matrix integral about a scalar:

$$\begin{aligned} \Pi(g, y + \psi) &= \Pi_0(g, y) + \frac{\Pi_1(g, y)}{N} \text{Tr } \psi \\ &+ \frac{1}{2} \left[\frac{\Pi_2(g, y)}{N} \text{Tr } \psi^2 + \frac{\Pi_{11}(g, y)}{N^2} (\text{Tr } \psi)^2 \right] \\ &+ \frac{1}{6} \left[\frac{\Pi_3(g, y)}{N} \text{Tr } \psi^3 + \frac{\Pi_{12}(g, y)}{N^2} \text{Tr } \psi \text{Tr } \psi^2 + \frac{\Pi_{111}(g, y)}{N^3} (\text{Tr } \psi)^3 \right] + \dots \end{aligned} \quad (16)$$

The vertex functions Π_p can be calculated explicitly, and are given in Appendix A. To understand what they are counting, we can expand several of them in powers of y :

$$\begin{aligned}
\Pi_0(g, y) &= \pi_0 + \pi_1 y + \frac{1}{2}(\pi_2 + \pi_{11})y^2 + \frac{1}{6}(\pi_3 + \pi_{12} + \pi_{111})y^3 + \dots \\
\Pi_2(g, y) &= \pi_2 + \left(\pi_3 + \frac{\pi_{12}}{3}\right)y + \frac{1}{2}\left(\pi_4 + \frac{\pi_{13}}{2} + \frac{\pi_{22}}{3} + \frac{\pi_{112}}{6}\right)y^2 + \dots \\
\Pi_3(g, y) &= \pi_3 + \left(\pi_4 + \frac{\pi_{13}}{4}\right)y + \dots, \text{ etc.} \tag{17}
\end{aligned}$$

The linear combinations of π_p 's in $\Pi_0, \Pi_2, \Pi_3, \dots$ are precisely those that occur in the low temperature expansion (4). The n -th coefficient of Π_0 counts clusters that have n external legs, each of which is connected to a tree, *i.e.*, none of its legs reconnect. By contrast, the n -th coefficient of Π_2 counts clusters that have two legs that lie on a loop (and will eventually reconnect), and n other legs that are connected to trees; and so on. Thus a cluster with three external legs, for example, may appear in the low temperature expansion as π_3 , $\pi_3 + \pi_{12}/3$, or $\pi_3 + \pi_{12} + \pi_{111}$, depending on whether it has 3, 2, or 0 legs that lie on loops.

The expansion of action (14) in powers of ψ is therefore⁷

$$\begin{aligned}
\frac{S_a}{\Delta} &= -N \left(\Pi_0 - \frac{y^2}{2a} + \rho y \right) - \rho \text{Tr } \psi + \frac{1}{2}(a^{-1} - \Pi_2)\text{Tr } \psi^2 - \frac{\Pi_{11}}{2N}(\text{Tr } \psi)^2 \\
&\quad - \frac{\Pi_3}{6}\text{Tr } \psi^3 - \frac{\Pi_{12}}{6N}\text{Tr } \psi \text{Tr } \psi^2 - \frac{\Pi_{111}}{6N^2}(\text{Tr } \psi)^3 + \dots \tag{18}
\end{aligned}$$

According to the above discussion, the vertex $\Pi_3 \text{Tr } \psi^3$ is really an infinite sum of vertices (17), and can be graphically represented as

$$\Pi_3(g, y) \text{Tr } \psi^3 \rightsquigarrow \begin{array}{c} \text{---} \\ \text{---} \\ \text{---} \end{array} + \begin{array}{c} \bullet \\ | \\ \text{---} \\ \text{---} \end{array} + \frac{1}{2} \begin{array}{c} \bullet \quad \bullet \\ \diagdown \quad \diagup \\ \text{---} \\ \text{---} \end{array} + \dots \tag{19}$$

while a non-linear vertex such as $\Pi_{12} \text{Tr } \psi \text{Tr } \psi^2$ may be represented as

$$\Pi_{12}(g, y) \text{Tr } \psi \text{Tr } \psi^2 \rightsquigarrow \begin{array}{c} \text{---} \\ \text{---} \\ \text{---} \end{array} + \begin{array}{c} \bullet \\ | \\ \text{---} \\ \text{---} \end{array} + \frac{1}{2} \begin{array}{c} \bullet \quad \bullet \\ \diagdown \quad \diagup \\ \text{---} \\ \text{---} \end{array} + \dots \tag{20}$$

⁷Two terms cancel due to (9).

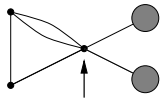
The model (18) is an expansion about the tree-like, mean field solution $\phi = y$. The geometrical meaning of this statement is reflected in the above pictures: trees are automatically included in the vertices of the new matrix model. The graphs of this matrix model can be pictured as a dense network (in fact, a spherical surface) of clusters, from the vertices of which sprout trees.

To proceed farther with the matrix model (18) we are obliged to truncate the potential $\Pi(g, y + \psi)$. The simplest possibility is to truncate after the quadratic term. We take $\rho = 0$ in this case, and immediately evaluate the partition function⁸

$$F = \Pi_0(y) - \frac{y^2}{2a} - \frac{1}{2\Delta} \log[1 - a\Pi_2(y)] - \frac{a\Pi_2(y)}{2\Delta} \quad (21)$$

The new $1/\Delta$ terms in the partition function just count the one-loop contributions to the low temperature expansion (4). It is clear that they cannot effect the critical behavior of the model: a large tree with one loop is indistinguishable from just a large tree. This can be demonstrated by noticing that the only way in which the $1/\Delta$ terms can effect the critical behavior of the model is through a divergence of the logarithm; but, since $\Pi_2 < \partial_y^2 \Pi_0 = \Pi_2 + \Pi_{11}$ (see Appendix A), and $1 - a\partial_y^2 \Pi_0 \geq 0$ in the physical region of the $q = \infty$ model (see [1]), this is impossible.

We are therefore obliged to keep higher order terms in the potential $\Pi(g, y + \psi)$. The meaning of a truncation after ψ^n terms, for $n \geq 3$, is as follows. Consider a cluster with λ links leading to other clusters. Of those links, λ_t are to trees and $\lambda_\ell = \lambda - \lambda_t$ are to loops; meaning that if one of the λ_t tree links is cut, the skeleton will be disconnected. For instance, the cluster indicated by the arrow

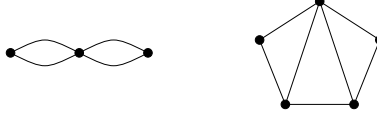


has $\lambda_t = 2$ and $\lambda_\ell = 3$. So: if we truncate the action (18) after the ψ^n terms, we discard any skeleton that has a cluster with $\lambda_\ell > n$. Note that λ_t does not matter: as discussed above, each vertex of (18) automatically includes arbitrary numbers of trees.

We now consider the model (18) in the *cubic approximation*: we discard all terms of order ψ^4 or higher. In this approximation the clusters—which

⁸The last term in (21) is there to cancel cluster self-connections; it should have been put in by hand as a constant in the action.

are themselves spherical φ^3 graphs—are arranged into spherical φ^3 graphs that also have trees of clusters growing from their vertices (given by powers of y : see (19), (20)). This structure will be called a “galaxy.” A typical graph in the cubic model has several galaxies, with the nonlinear terms $(\text{Tr } \phi)^2$, $\text{Tr } \phi \text{Tr } \phi^2$, and $(\text{Tr } \phi)^3$ connecting the galaxies into a tree structure (not to be confused with the trees that grow out of the vertices inside the galaxies). The cubic approximation differs radically from the quadratic one in that it does not simply sum over graphs with one more loop and with one higher order in Δ^{-1} , but rather it sums over a large class of graphs with an arbitrary number of loops. In fact, it sums over all graphs, provided that no cluster has more than three legs lying on loops; for example, the following are simple skeleton graphs that are *not* included in the cubic approximation:



The solution of the cubic model will proceed along the same lines as the simpler model solved in [13]. First off, we set

$$\rho = -\frac{\Pi_3}{2a} - \frac{\Pi_{12}}{6a} \quad (22)$$

to cancel the cluster self-connections. Then we follow the standard procedure, reducing the problem to eigenvalues and introducing a continuous approximation to the spectrum $\lambda(x)$. Using procedure that is exact in the $N \rightarrow \infty$ limit we introduce the two moments

$$c = \left\langle \frac{1}{N} \text{Tr } \psi \right\rangle = \int dx \lambda(x), \quad d = \left\langle \frac{1}{N} \text{Tr } \psi^2 \right\rangle = \int dx \lambda^2(x) \quad (23)$$

as parameters, for which will we solve self-consistently at the end. The saddle point equation for the action reads

$$\frac{\delta S}{\delta \lambda} = q + m\lambda(x) + 3p\lambda^2(x) - \frac{1}{2} \int' \frac{dy}{\lambda(x) - \lambda(y)} = 0 \quad (24)$$

$$-\frac{p}{\Delta} = \frac{\Pi_3}{6} \quad (25)$$

$$-\frac{m}{\Delta} = -\frac{1}{a} + \Pi_2 + \frac{c\Pi_{12}}{3} \quad (26)$$

$$-\frac{q}{\Delta} = \rho + c\Pi_{11} + \frac{d\Pi_{12}}{6} + \frac{c^2\Pi_{111}}{2} \quad (27)$$

keeping in mind that the Π_p 's are (complicated) functions of g and $y(g, a)$. The eigenvalue density for this problem is

$$u(\lambda) = \frac{1}{\pi}(m + \sigma + 3p\lambda)\sqrt{\frac{4}{m + 2\sigma} - \left(\lambda - \frac{\sigma}{3p}\right)^2} \quad (28)$$

where the variable σ satisfies the equation

$$18p^2 + \sigma(m + \sigma)(m + 2\sigma) + 3pq(m + 2\sigma) = 0 \quad (29)$$

Using the eigenvalue density (28), the self-consistency conditions on c and d become

$$c = \frac{3p}{(m + 2\sigma)^2} + \frac{\sigma}{3p} \quad (30)$$

$$d = \frac{m + 4\sigma}{(m + 2\sigma)^2} + \left(\frac{\sigma}{3p}\right)^2 \quad (31)$$

The reader is reminded that the eigenvalue density (28) is for the ψ matrix. Since σ scales as Δ^0 , for large Δ the eigenvalue density for ϕ in the cubic approximation is centered on the $q = \infty$ value y with a displacement $\sigma/3p \sim \mathcal{O}(\Delta^{-1})$. The width of the distribution is $\sqrt{4/(m + 2\sigma)} \sim \mathcal{O}(\Delta^{-1/2})$, as previously advertised.

4 Critical behavior

The cubic approximation to the Potts model is expected to have three critical phases: the phase of *large clusters*, the phase of *large trees* of clusters, and the phase of *large galaxies* of clusters.

First, the regime of *large clusters*. This is the magnetized, low temperature phase. As we have an approximate form for the eigenvalue density (28), we can plug it back into the full action (12) and look for the singularities of the potential $\Pi(g, \phi)$. The reader is reminded [2] that for $q = \infty$, the eigenvalue density is a delta function at $y(g, a)$; the potential in that case can easily be reduced to the “standard” form $\phi^2/2 + G\phi^3$, with $G = (1 - 12gy)^{-3/4}g$. At the critical point

$$G = G_c = 1/\sqrt{108\sqrt{3}} \quad (32)$$

the area of the clusters (but not their number) diverges. The same thing happens in the case of the spread out density (28), though the computation is

somewhat more difficult: we are looking for the critical point of the external matrix model (6). The result can be found in [14]. The only dependence on the external matrix is through the moments

$$\sigma_k = \int d\lambda u(\lambda)(x - \lambda)^{-k/2} \quad (33)$$

where the variable x satisfies the implicit equation

$$x = \frac{1}{12g} - \sqrt{3g}\sigma_1(x) \quad (34)$$

For the eigenvalue density, these moments can be calculated explicitly (as functions of x):

$$\begin{aligned} \sigma_k = & \left(x - y - \frac{\sigma}{3p}\right)^{-k/2} \left[{}_2F_1\left(\frac{1}{2} + \frac{k}{4}, \frac{k}{4}; 2; \frac{4}{(1+2\sigma)(x-\sigma/3p)^2}\right) \right. \\ & \left. + \frac{3kp}{2(1+2\sigma)^2(x-\sigma/3p)} {}_2F_1\left(\frac{1}{2} + \frac{k}{4}, 1 + \frac{k}{4}; 3; \frac{4}{(1+2\sigma)(x-\sigma/3p)^2}\right) \right] \end{aligned} \quad (35)$$

The criticality condition is the point where the x equation (34) ceases to have solutions. Algebraically this can be expressed as

$$3g\sigma_3^2 = 4 \quad (36)$$

It can easily be checked that when $q, \Delta \rightarrow \infty$, and consequently $\sigma/3p, 4/(m+2\sigma) \rightarrow 0$, these new criticality conditions (34) and (36) reduce to (32). It will be seen in the phase diagrams that as q approaches infinity, the curve of large clusters will approach the corresponding $q = \infty$ curve, given by solving eqs. (32) and (10) simultaneously.

In the large cluster phase matter is manifestly magnetized, and is therefore decoupled from the geometry; so this is a phase of pure gravity, with $\gamma_{\text{str}} = -\frac{1}{2}$. Another way of saying the same thing: in this phase the number of clusters is small, and few clusters is the same as one cluster, as far as critical behavior is concerned.

Second, the phase of *large trees* of clusters. There are, in principle, two ways of getting there. At $q = \infty$, the trees become large when the saddle point equation for $y(g, a)$ (10) ceases to have a solution [2]; in other words, when

$$a \frac{\partial^2}{\partial y^2} \Pi(g, y) = a [\Pi_2(g, y) + \Pi_{11}(g, y)] = 1 \quad (37)$$

The other way to get large trees is to make the tree of *galaxies* (of clusters) blow up. This is not exactly the same as a large tree of clusters at $q = \infty$, but very nearly the same, as in general the galaxies at the vertices of this tree will be small; and as far as critical behavior is concerned, a small galaxy is no different from a galaxy of size one, in other words, a single cluster. This intuition is supported by the fact that both large tree phases have $\gamma_{\text{str}} = +\frac{1}{2}$; and as $q \rightarrow \infty$, the curves of the two phases approach each other.

To calculate the location of the second large tree phase, we can look for the point in the cubic model (24) where the string susceptibility $\partial^2 F / \partial p^2$ diverges [13]. Equivalently, and computationally simpler, we can look for the divergence of the “pseudo-susceptibility”⁹

$$c' \equiv \frac{\partial c}{\partial p} \rightarrow \infty \tag{38}$$

This is most simply done by differentiating the eqs. (29–31) with respect to p , and solving the resulting linear system for c' , d' , and σ' . As the result is unwieldy, and in any case can easily be derived, it will not be given here. The same procedure, if applied to the simple quartic model in [13], reproduces the result for the large tree phase given in that work.

In the large tree phase one has an ensemble of clusters of different size. As one moves toward the magnetized phase, clusters of higher and higher area begin to be included. At the multicritical point, some moments of the cluster area diverge, a sign of a continuous spin ordering phase transition.¹⁰ The susceptibility exponent in the bulk of the tree phase is $\gamma_{\text{str}} = \frac{1}{2}$, the generic exponent for tree growth. In the tree phase, and only in the tree phase, the clusters are probably identical to the geometric structures known as “baby universes” [8]. Therefore the transition to large trees from high temperature can be interpreted as a magnetization of baby universes (but not of the whole surface); and the transition to trees from low temperature can be interpreted as a break-up of the magnetized surface into magnetized (but in different directions) baby universes [9].

Finally, the cubic model should also have a phase of *large galaxies*. This occurs simply at the normal, BIPZ, critical point of the model (24). This is

⁹ d' or σ' would do just as well.

¹⁰ For the Ising model on a fixed two-dimensional lattice, for example, the second moment of the cluster size distribution is the lowest one to diverge.[15]

simply given by

$$\Gamma = \frac{p}{(m - 12pq)^{3/4}} = \Gamma_c = \frac{1}{\sqrt{108\sqrt{3}}} \quad (39)$$

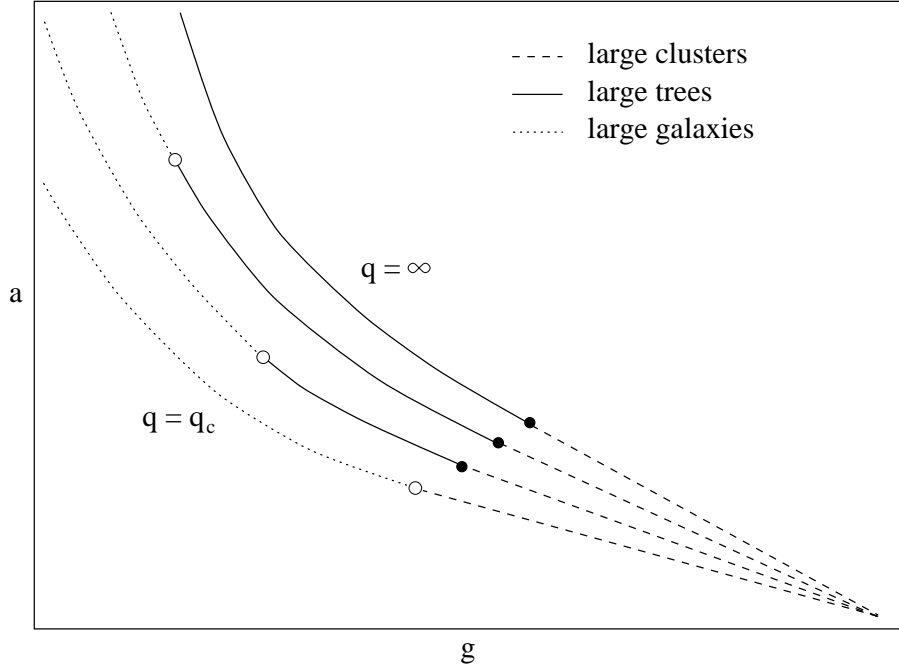
This phase is radically different from anything that exists at $q = \infty$; it is in this phase that loops become important. Interestingly, it bears some resemblance to what *must* be the case for small q : the spin clusters at high temperature do not form trees, but complicated planar networks with many loops.

The large planar networks of clusters in the galaxy phase resemble the configurations of a low q model at high temperature. As we go to higher temperature, moreover, the clusters get smaller, as matter fluctuations are once again decoupled from the geometry. The large galaxy phase is therefore pure gravity, once again. The susceptibility exponent is $\gamma_{\text{str}} = -\frac{1}{2}$, the standard pure gravity value for nonlinear models in this phase.

We are now ready to study the complicated transcendental equations of the cubic approximation. The procedure is as follows. First, fix the three adjustable parameters: $\Delta = q - 1$, g , and a . Then solve the saddlepoint equation (10) for $y(g, a)$; this fixes all coefficients in the cubic action (18). Next, solve the cubic equation (30) for c as a function of σ , plug into (29) and solve numerically for σ , taking the root closest to zero. Finally, check the criticality conditions: (34) and (36) for the phase of large clusters; (38) for large trees; or (39) for large galaxies.

The following is a schematic, not-to-scale sketch of the resulting critical

curves.

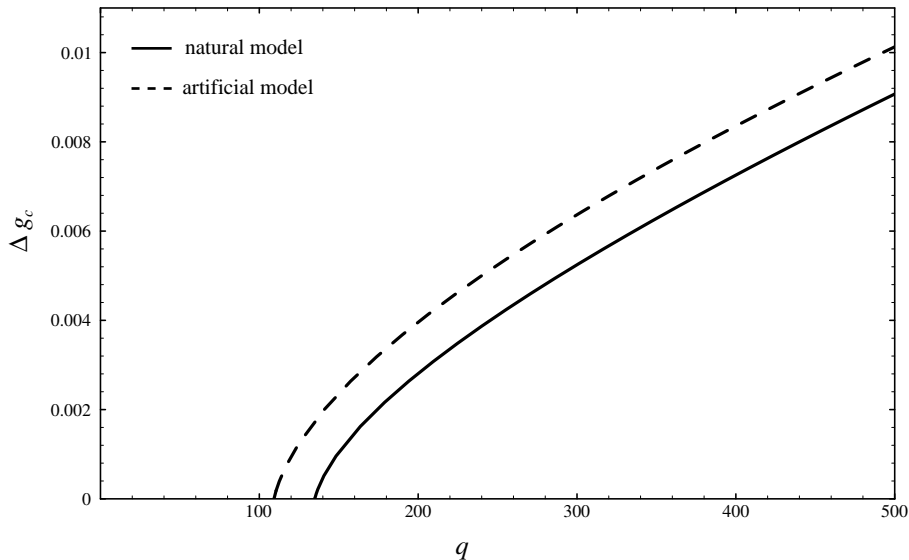


If drawn to scale, the curves are rather close to each other and hard to distinguish by eye. As $q \rightarrow \infty$, the curves reassuringly approach the exact $q = \infty$ critical curve, where the transition from magnetized to tree phases occurs at $g = 1/\sqrt{288}$, $a = 1$. As we move away from $q = \infty$, the new critical regime of large galaxies appears. As q gets lower, the phases of large galaxies and large clusters approach each other, eating away at the mean field, large tree phase.

The susceptibility exponent γ_{str} is $-\frac{1}{2}$ in the magnetized and galaxy phases, as discussed above, and $+\frac{1}{2}$ in the tree phase. At the two multicritical points $\gamma_{\text{str}} = \frac{1}{3}$. Further, we find $\alpha = -1$ at both multicritical points, as shown in Appendix C. The equality of the exponents at the two multicritical points is not a coincidence: the model at one of the points can be mapped onto the model at the other—see the appendix for details.

At $q = q_c$ ($q_c \approx 133$ for the natural model, and $q_c \approx 108$ for the artificial model), the phase of large trees ceases to exist. Thereafter, the magnetized phase of large clusters goes directly into a phase of large galaxies. The mean field behavior is entirely eliminated. Let $g_{c1}(q)$ be the multicritical point between phases of large galaxies and large trees, and $g_{c2}(q)$ the multicritical

point between the phases of large trees and large clusters. $\Delta g_c = g_{c2} - g_{c1}$ is a measure of “how much of mean field theory is left” at a given value of q . Here it is plotted for both the natural and the artificial models.



For $q \leq q_c$, the two pure gravity phases (magnetized and large galaxies) are joined directly onto each other, with a multicritical point in the middle. This phase diagram bears a striking resemblance to the known phase diagram for, say, $q = 2$ [16].

5 Discussion

The results obtained for q_c cannot be considered as anything more than order-of-magnitude estimates. The real result of this calculation is the discovery of the mechanism for the break-down of mean field theory: the divergence of galaxies. The resulting critical behavior interpolates smoothly

between the somewhat odd phase diagram at $q = c = \infty$ and the well-known phase diagram for $q \leq 4, c \leq 1$. Another result of this calculation is the likelihood that q_c is *finite*, that mean field behavior holds for some finite Potts models (with modifications, as has been shown).

The two natural questions at this stage are: is the present result merely an artifact of the truncation of the action (18), or are the higher-order terms essential? And does a similar picture hold for conformally symmetric models, which, after all, reduce to the same mean field theory at $c = \infty$?

The first question should not be too hard to answer. It seems that we would not find any qualitatively new behavior by including the higher-order terms, which would simply add other types of vertices to the galaxies but would not modify the essential structure. Mean field theory should always be destroyed by the divergence of the galaxies. It is true that quartic or higher models will add new multicritical points; but as we only have the three parameters q, g , and a to tune, we should not be able to reach them. To repeat the present calculation in the quartic approximation should be somewhat tedious, but not too difficult.

The second question is more difficult to answer, and the author does not have any suggestions on how to deal with it. The immediate difficulty is that, although effective cluster models such as (11) and (12) can be introduced for any matter model on the surface, they are multi-matrix rather than one-matrix models. Still, they closely resemble the $c = \infty$ model, so perhaps it is the right way to start.

The author thanks the Niels Bohr Institute for its hospitality, and Jan Ambjørn and Gudmar Thorleifsson for stimulating discussions. Marc Potters provided many of the ideas in the early stage of this work.

Appendix A

Here we give expressions for the first few Green's functions $\pi_p(g)$ in the expansion (7) of the external matrix integral $\Pi(g, \Lambda)$, defined in (6). Using Gross and Newman's notation, the external matrix integral is

$$\begin{aligned} \Pi(g, \Lambda) = & -\frac{1}{2N^2} \sum_{a,b} \log(\mu_a + \mu_b) - \frac{1}{6g}(\sigma_{-2} - x) + \frac{2}{\sqrt{27g}}\sigma_{-3} \\ & + \sigma_1\sigma_{-1} + \sqrt{\frac{g}{48}}\sigma_1^3 - \frac{1}{108g^3} - \frac{1}{4}\log 3g \end{aligned} \quad (40)$$

where the λ_a are eigenvalues of Λ , $\mu_a = \sqrt{x - \lambda_a}$, $\sigma_k = \frac{1}{N} \sum_a (x - \lambda_a)^{-k/2}$, and the variable x satisfies the implicit equation (34).

First we expand x in powers of Λ :

$$x = x_0 - \frac{\sqrt{3g}}{\sqrt{3g} - 2x_0^{3/2}} \frac{\text{Tr } \Lambda}{N} \quad (41)$$

$$- \frac{9g (\sqrt{3g} - 4x_0^{3/2})}{4x_0 (\sqrt{3g} - 2x_0^{3/2})^3} \frac{(\text{Tr } \Lambda)^2}{N^2} + \frac{3\sqrt{3g}}{4x_0 (\sqrt{3g} - 2x_0^{3/2})} \frac{\text{Tr } \Lambda^2}{N} + \dots$$

where x_0 satisfies the cubic equation

$$x_0 = \frac{1}{12g} - \sqrt{\frac{3g}{x_0}} \quad (42)$$

$$= \frac{1}{18g} + \frac{1}{36} \left(\sqrt{3} \sin \frac{2\theta}{3} - \cos \frac{2\theta}{3} \right) \quad (43)$$

$$\tan \theta = \sqrt{\left(\frac{g_0}{g}\right)^4 - 1}, \quad g_0 = \frac{1}{\sqrt{108\sqrt{3}}}$$

$$= \frac{1}{12g} - 6g - 216g^3 - \dots$$

Plugging the series for x back into (40), after some algebra we find

$$\pi_1 = \sqrt{\frac{x_0}{3g}} + \frac{1}{4x_0} - \frac{1}{6g}$$

$$= 3g + 108g^3 + 7776g^5 + \dots$$

$$\pi_2 = \frac{1}{2\sqrt{3g}x_0} - \frac{1}{16x_0^2} - 1$$

$$= 27g^2 + 1944g^4 + \dots$$

$$\pi_{11} = \frac{1}{16x_0^2}$$

$$= 9g^2 + 1296g^4 + \dots$$

$$\pi_3 = \frac{1}{4\sqrt{3g}x_0^{3/2}} - \frac{1}{16x_0^3}$$

$$= 6g + 540g^3 + 58320g^5 + \dots$$

$$\pi_{12} = \frac{3}{16x_0^3}$$

$$\begin{aligned}
&= 324g^3 + 69984g^5 + \dots \\
\pi_{111} &= \frac{3g}{8x_0^3(4x_0^3 - 3g)} + \frac{\sqrt{3g}}{4x_0^{3/2}(4x_0^3 - 3g)} \\
&= 7776g^5 + \dots
\end{aligned}$$

The corresponding coefficients Π_p in the expansion of $\Pi(g, y + \Lambda)$ (16) can be obtained in a similar manner. The above expressions for $\pi_p(g)$ go directly into $\Pi_p(g, y)$ with the substitution $x_0 \rightarrow x_0 - y$, while x_0 itself now satisfies

$$x_0 = \frac{1}{12g} - \sqrt{\frac{3g}{x_0 - y}} \quad (44)$$

and is given by

$$\begin{aligned}
x_0 &= \frac{1}{18g} + \frac{y}{3} + \frac{1 - 12gy}{36} \left(\sqrt{3} \sin \frac{2\theta}{3} - \cos \frac{2\theta}{3} \right) \\
\tan \theta &= \sqrt{\left(\frac{g_0}{G} \right)^4 - 1}, \quad G = \frac{g}{(1 - 12gy)^{3/4}}
\end{aligned} \quad (45)$$

Appendix B

Consider a model with an extra matrix ϕ and the action

$$S' = \text{Tr} \left(\phi \sum_i \phi_i - \frac{1}{2b_q} \phi^2 + \frac{a_q - b_q}{2} \sum_i \phi_i^2 + g \sum_i \phi_i^3 \right) \quad (46)$$


with a_q, b_q given in (3). On one hand, the extra matrix can be integrated out to give exactly the model (1); on the other hand, the ϕ_i can be integrated out in (46) to give a one-matrix model with the action

$$S_n = \Delta \left[\frac{1}{2\hat{a}} \text{Tr} \phi^2 - N \left(1 + \frac{1}{\Delta} \right) \Pi \left((1 - a/\Delta)^{3/2} g, \phi \right) \right], \quad \hat{a} = \frac{a}{1 - a/\Delta} \quad (47)$$

Whereas the vertices of the original multi-matrix model (1) are the points of a discretized worldsheet, the vertices of the effective one-matrix model (47) are spin clusters.

The partition function of the effective one-matrix model (47) can be expanded in powers of a (not \hat{a}) to reproduce the low temperature expansion given above (4). The reason that this works is that a vertex like $(\text{Tr} \phi)^2$, such as occurs in the action (47), is equivalent—as far as large N behavior

is concerned—to a twisted cluster, as explained in the text. The correspondence between the two expansions is still not completely trivial, because in the low temperature expansion (4)

- the propagator between clusters is a , rather than \hat{a} ;
- a cluster is never linked to itself—by definition;
- the coefficient of a skeleton graph is a polynomial in Δ^{-1} , whose leading term is $\Delta^{v-\ell-1}$ (where v and ℓ are the numbers of vertices and links in the graph)¹¹; if there are no loops of length greater than two present, the polynomial is just a monomial, but otherwise there are subleading terms that arise due to the finite volume of target space—for instance, the coefficient of  is $\Delta^{-1}(1 - \Delta^{-1})$.

Evidently, the $1/\Delta$ terms in the action (47)—the correction to the coefficient of Π and the renormalization $g \rightarrow (1 - a/\Delta)^{3/2}g$ —conspire to compensate for the above three discrepancies.

In the calculation to be performed, the potential Π in the effective one-matrix model (47) will be truncated after the cubic term (only the terms written out in equation (7) are included). It is instructive to consider the effect of this truncation on the low temperature expansion of the effective model. Of course the clusters will now have no more than three neighbors. Furthermore, consider, say, the coefficient of a^2 :

$$\frac{1}{2}\pi_1^2(\pi_2 + \pi_{11}) + \frac{1}{4\Delta}\pi_2^2 - \frac{1}{12\Delta^2}\left(\pi_4 + \frac{\pi_{22}}{2}\right) \quad (48)$$

The first two terms reproduce the low temperature expansion (4). The last term, however, compensates for the tadpole

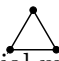


that would have been generated by the ϕ^4 terms. This over-compensation for tadpoles is somewhat undesirable. We can consider an alternate, “artificial” action (as opposed to the “natural” action (47))

$$S_a = \Delta \left[-\rho \text{Tr} \phi + \frac{1}{2a} \text{Tr} \phi^2 - N\Pi(g, \phi) \right] \quad (49)$$

¹¹Assuming that the expansion (4) is rewritten in terms of a , rather than c

with ρ adjusted to cancel the simple tadpoles (*i.e.*, the cluster self-connections), in this case to $-(\pi_1 + \pi_3/2 + \pi_{12}/6)a$. Strictly speaking, a constant term should also be added to S_a to cancel *all* the cluster self-connections; but as this term will have no effect whatsoever on the calculations here, it will be omitted. The partition function of the artificial model, when expanded in low temperature series, reproduces the low temperature expansion (4) exactly, *except* that the coefficient of each graph is precisely $\Delta^{v-\ell-1}$, so that

the coefficient of , for example, is Δ^{-1} rather than the correct $\Delta^{-1}(1 - \Delta^{-1})$. The artificial model (49) does not know about the target space of the original Potts model, and so it cannot reproduce its excluded volume effects. On the positive side, the potential Π in the artificial action can be truncated at any point without introducing tadpole overcompensation terms such as (48).

To summarize, there are two effective one-matrix models for the Potts model, the “natural” model (47) and the closely related “artificial” model (49). If the potential $\Pi(\phi)$ in these models is truncated, slight discrepancies (different for the two models) are introduced into their low temperature expansions, as compared to the series (4). These discrepancies are not important when q is large. For instance, the critical behavior of the natural and artificial models is identical, up to slightly different critical parameter values.

Appendix C

Here we sketch the calculation of the critical exponent α . It is defined by the singular behavior of the partition function $F \sim |g - g_c|^{2-\alpha}$, where we constrain the approach to the multicritical points to lie on a critical curve.

At $q = \infty$, we can calculate α exactly for the multicritical point between the large tree phase and the magnetized pure gravity phase. The partition function F_∞ is given by eqs. (9) and (10). The multicritical point occurs at $g_* = 1/\sqrt{288}$, $a_* = 1$. We vary g , and constrain a to lie on the critical curve. When $g > g_*$, this is given by

$$a_+(g) = \frac{1 - (g/g_0)^{4/3}}{1 - \sqrt{3}(g/g_0)^{2/3} + (g/g_0)^{4/3}} \quad (50)$$

where $g_0^2 = 1/108\sqrt{3}$ is the pure gravity critical point; when $g < g_*$, the

critical curve is given by the equation (37)

$$a_- \frac{\partial^2}{\partial y^2} \Pi(g, y) = a_- [\Pi_2(g, y) + \Pi_{11}(g, y)] = 1 \quad (51)$$

in conjunction with eq. (9). The partition function turns out to be analytic on either side of the multicritical point. Putting $\Delta g = g - g_*$, and using the expressions given in Appendix A, we find

$$F_+(g) \equiv \lim_{g \searrow g_*} F_\infty(g, a_+(g)) = \left(\frac{7}{24} - \frac{1}{2} \log 2 \right) + 96\Delta g^2 - 2432\sqrt{2}\Delta g^3 + \dots$$

$$F_-(g) \equiv \lim_{g \nearrow g_*} F_\infty(g, a_-(g)) = \left(\frac{7}{24} - \frac{1}{2} \log 2 \right) + 96\Delta g^2 - 5760\sqrt{2}\Delta g^3 + \dots$$

The discontinuity in the third derivatives means that the transition is of third order, with $\alpha = -1$. The corresponding transition from the magnetized to the tree phase for $\infty < q < q_c$ is similar, and should have the same exponents.

At the other multicritical point, the boundary between the tree and galaxy phases, the geometric fluctuations of the clusters (as given by the coefficients Π_p in action (18)) no longer matter; what drives the transition is the *inter*-cluster dynamics of the galaxies, as well as the inter-galaxy dynamics. To calculate the critical exponent we therefore may ignore the complexities of the coefficients $\Pi_p(g, y)$ in the action, and consider any simple non-linear matrix model which displays similar behavior. As a first example, take the quartic model

$$S = \text{Tr} \left(\frac{1}{2} \phi^2 + g \phi^4 \right) + \frac{g'}{N} (\text{Tr} \phi^2)^2 \quad (52)$$

that was solved in [13]; the exponent α has never been given in the literature.¹² The phase of “large galaxies” ($\gamma_{\text{str}} = -\frac{1}{2}$) occurs on the curve $g' = g'_-(g)$ and the phase of large trees ($\gamma_{\text{str}} = +\frac{1}{2}$) occurs on the curve $g' = g'_+(g)$, with

$$g'_+ = -g - \frac{1}{32} \left(1 + \sqrt{1 + 64g} \right) \quad (53)$$

$$g'_- = -9g - \frac{3}{4} \sqrt{-3g} \quad (54)$$

¹²In the context of the original work [13], this exponent is meaningless, as there is no outright matter coupled to the surface.

The multicritical point occurs at $g_* = -3/256, g'_* = -9/256$. As above, we fix $g' = g'_\pm$ and find on either side of the multicritical point

$$F_+ = \left(\frac{29}{72} - \frac{1}{2} \log \frac{8}{3} \right) - \frac{64}{27} \Delta g + \frac{8192}{27} \Delta g^2 + \frac{8388608}{243} \Delta g^3 + \dots$$

$$F_- = \left(\frac{29}{72} - \frac{1}{2} \log \frac{8}{3} \right) - \frac{64}{27} \Delta g + \frac{8192}{27} \Delta g^2 - \frac{8388608}{243} \Delta g^3 + \dots$$

Therefore the transition is again of third order, with $\alpha = -1$.

As another example, consider the nonlinear cubic model

$$S = \text{Tr} \left(\frac{1}{2} \phi^2 + g \phi^3 \right) + \frac{g'}{2N} (\text{Tr} \phi)^2 \quad (55)$$

which is closer to our effective model, eq. (18). Of course it has exactly the same critical behavior as the quartic model (52), which can be shown in an identical manner. It is more instructive, however, to consider the partition function of the model (55) directly: it is simply given by

$$F = \Pi(g, cg') - \frac{g' c^2}{2} \quad (56)$$

where c is the one-point function, given by the self-consistency condition

$$c = \left\langle \frac{1}{N} \text{Tr} \phi \right\rangle = \Pi_1(g, cg') \quad (57)$$

exactly analogous to (30). If we put $y = cg'$, we obtain precisely the partition function of the $q = \infty$ model (9), along with its saddle point condition, eq. (10). Therefore $\alpha = -1$, as calculated above.

We have therefore mapped one of the multicritical points onto the other. A similar mapping holds for the full action (18), giving $\alpha = -1$ at the transition between the tree and galaxy phases. This mapping points up the similarity of the magnetized phase to the phase of large galaxies: in the former the individual clusters blow up, while in the latter it is galaxies of clusters that diverge. Both phases are, essentially, pure gravity.

References

- [1] M. Wexler, *Nucl. Phys.* **B410** (1993) 377.
- [2] M. Wexler, *Mod. Phys. Lett.* **A8** (1993) 2703.

- [3] M. Wexler, *Phys. Lett.* **315B** (1993) 67.
- [4] J. Ambjørn, B. Durhuus, T. Jónsson, ‘A solvable 2-d gravity model with $\gamma > 0$ ’, Niels Bohr Institute preprint NBI-HE-94-02, hep-th@xxx.lanl.gov/9401137.
- [5] B. Durhuus, ‘Multi-spin systems on a randomly triangulated surface’, Copenhagen Univ. preprint KUMI-94-2, hep-th@xxx.lanl.gov/9402052.
- [6] L. Alvarez-Gaumé, J. L. F. Barbón and C. Crnković, *Nucl. Phys.* **B394** (1993) 383.
- [7] M.G. Harris and J.F. Wheeler, ‘Multiple Ising spins coupled to 2d quantum gravity’, Oxford preprint OUTP-9407P, hep-th@xxx.lanl.gov/9404174.
- [8] J. Ambjørn, S. Jain and G. Thorleifsson, *Phys. Lett.* **307B** (1993) 34; J. Ambjørn and G. Thorleifsson, *Phys. Lett.* **323B** (1994) 7.
- [9] J. Ambjørn, J. Jurkiewicz, G. Thorleifsson and M. Wexler, in preparation.
- [10] P. Ginsparg and G. Moore, ‘Lectures on 2D gravity and 2D string theory.’ Yale preprint YCTP-P23-92, Los Alamos preprint LA-UR-92-3479 (1992).
- [11] E. Brézin, C. Itzykson, G. Parisi and J.-B. Zuber, *Commun. Math. Phys.* **59** (1978) 35.
- [12] V.A. Kazakov, *Nucl. Phys. B* (Proc. Suppl.) **4** (1988) 93.
- [13] S.R. Das, A. Dhar, A.M. Sengupta and S.R. Wadia, *Mod. Phys. Lett.* **A5** (1991) 1041.
- [14] D.J. Gross and M.J. Newman, *Phys. Lett.* **266B** (1991) 291.
- [15] M.E. Fisher, *Physics* **3** (1967) 255.
- [16] V. A. Kazakov, *Phys. Lett.* **119A** (1985) 140.